Pergamon

Journal of Structural Geology, Vol. 18, No. 11, pp. 1327 to 1343, 1996

PII: S0191-8141(96)00057-0
0191-8141/96 $15.00 + 0.00

Deformation partitioning during updoming of the Sonnblick area in the Tauern Window (Eastern Alps, Austria)

WALTER KURZ and FRANZ NEUBAUER

Institut für Geologie und Paläontologie, Paris-Lodron-Universität Salzburg, Hellbrunner Straße 34, Salzburg, Austria

(*Received* 21 *November* 1994; *accepted in revised form* 8 *July* 1996)

Abstract—The Sonnblick Dome forms a NE-vergent dome structure cored by basement gneisses within the southeastern Tauern Window of the Eastern Alps (Austria). A succession of ductile and brittle deformation stages documents doming and exhumation subsequent to the thermal peak of metamorphism. Contrasting deformation geometries within internal parts and along the margins of the dome are explained in terms of deformation partitioning. Subhorizontal shortening is documented by subvertical en-echelon extensional gashes within central parts of the dome. Subhorizontal as well as subvertical flattening is also documented by fold structures. During dextral transpression strike-slip is accommodated along the NE margin (Sonnblick Lamella, Möll Valley Fault) and the southern margin (Moser Fault) of the Sonnblick Dome, while vertical thickening occurred within the interior of the dome. Crustal thickening triggered unroofing and extension parallel to the dome axis which is documented by ductile low-angle normal faults in the uppermost structural sections of the dome. This normal fault system contributed to footwall uplift and exhumation of the dome structure. The Sonnblick Lamella, associated with the dextral Möll Valley Fault, forms a stretching fault where deformation is concentrated along a potential zone of weakness. This fault is interpreted to represent the transition from vertical thickening within the dome to vertical thinning at the dome margins. During upbending, the dome structure passed the isotropic stress surface that is characterized by equality of σ_1 and σ_2. This is documented in a perturbation of the orientations of principal stress axes σ_1 and σ_2, while σ_3 remains constant in orientation. Transpression contributed substantially to updoming and to rapid, nearly isothermal, exhumation subsequent to the thermal peak of metamorphism. Copyright © 1996 Elsevier Science Ltd

INTRODUCTION

The exhumation history of metamorphic core complexes within internal zones of collisional orogens has been intensively studied in the last decades (Coney 1980, Davies 1983, Lister *et al.* 1984, Malavielle 1987, Lister & Davis 1989, Behrmann & Frisch 1990). Additionally, petrological and geochronological investigations allow the reconstruction of exhumation and cooling rates of rocks exposed within metamorphic core complexes (Selverstone 1985, 1993, Selverstone & Spear 1985, Neubauer *et al.* 1995). Apparently exhumation occurs mainly during late overall contractional stages of orogenic evolution in a local extensional regime (Platt 1986, Dewey 1988, Ratschbacher *et al.* 1989, England & Molnar 1990, Hill & Baldwin 1993, Platt 1993). Removal of hanging-wall crust is achieved by downward displacement along ductile low-angle normal faults that are directed either towards the foreland (Lister *et al.* 1984) or subparallel to the orogen (Behrmann 1988, 1990, Selverstone 1988, Ratschbacher *et al.* 1989, 1991, Neubauer *et al.* 1995). While the geometry and development of these low-angle normal faults is well investigated (Behrmann 1988, Genser & Neubauer 1989, Lister & Davis 1989, Hill *et al.* 1992), the lateral boundaries of these detachment surfaces, and the deformation in the inner parts of the exhumed domes have been neglected.

The exhumation history of the metamorphic Penninic units within the Tauern Window in the Eastern Alps (Figs. 1a & b) is well-constrained by petrological and geochronological data (Selverstone *et al.* 1984, 1991, Cliff *et al.* 1985, Droop 1985, Selverstone 1985, 1988, 1993, Selverstone & Spear 1985, Christensen *et al.* 1994). These data indicate a nearly isothermal exhumation rate of up to 5 mm per year subsequent to the peak temperature of metamorphism. We discuss here a tectonic mechanism that can explain these high exhumation rates within the Tauern Window, which are near or beyond the highest exhumation rates that occur due to erosional denudation. In particular, we investigated the southeastern part of the Tauern Window to obtain information on (1) the interaction of extension parallel to the dome-axis with exhumation, (2) structural boundary conditions during the formation of metamorphic domes, and (3) different deformation paths within the interior and along the margins of an upbending dome structure.

GEOLOGICAL SETTING

The Tauern Window (Fig. 1) exposes Penninic units below the Austroalpine Nappe Complex which represents the hanging-wall continental plate during Upper Cretaceous and Lower Tertiary plate collision. The Penninic units include the widely distributed Zentralgneis comprising deformed Variscan granitoids, and a lower continental basement complex of Paleozoic metamorphic units with a parautochthonous cover (the Lower Schieferhülle). The basement complex is considered to represent a duplex of European continental crust. The Zentralgneis is exposed in a series of domes within the Tauern Window, such as the Zillertal–Venediger Dome and the Hochalm Dome (Fig. 1b). The Peripheral Schieferhülle comprises several nappes with the Glockner

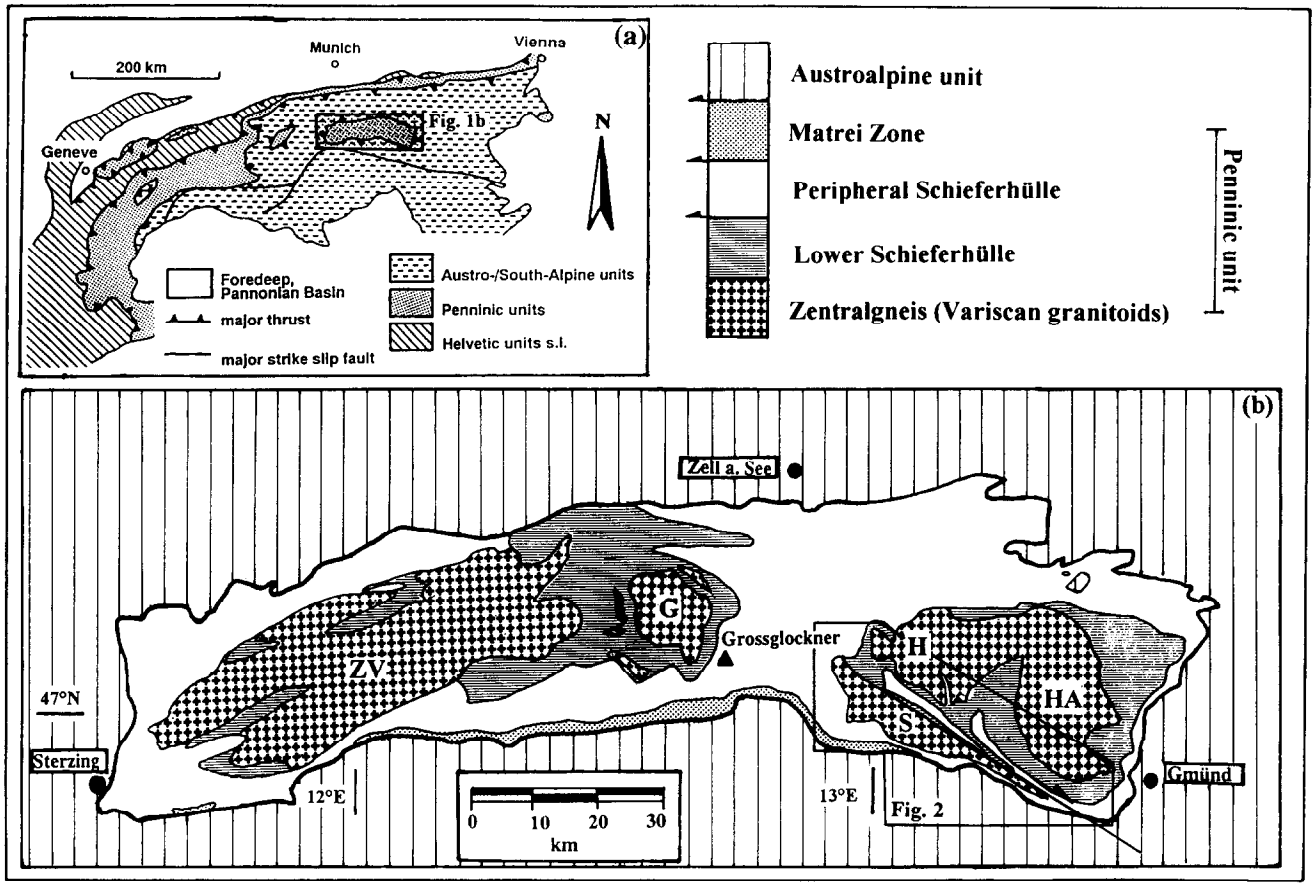

Fig. 1. (a) Location of the Tauern Window within the Alps. (b) Tectonic sketch map of the Tauern Window (after Tollmann 1977); S—Sonnblick Dome; HA—Hochalm-Ankogel Dome; H—Hölltor-Rotgülden Dome; G—Granatspitz Dome; ZV—Zillertal—Venediger Domes.

Nappe forming the suture zone between the Austroalpine and the remaining Penninic units (Bickle & Hawkesworth 1978, Behrmann 1990, Kurz *et al.* 1996).

The basement units in the southeastern Tauern Window are exposed within the Hochalm–Ankogel and the Sonnblick Domes, which are separated by the Mallnitz Synform. This synform exposes Permian to Mesozoic metasedimentary/metavolcanic rocks of the Schieferhülle (Figs. 2a and 3). The Sonnblick Dome forms a large NE-vergent antiformal dome structure that narrows dramatically to the southeast to form the Sonnblick Lamella (Exner 1962, 1964, Cliff *et al.* 1971) (Figs. 1, 2a & 3). The Sonnblick Lamella is reduced to a thickness of 100–300 m and can be traced to the SE for *ca.* 20 km (Figs. 2a & 3). The Knappenhauswalze (Fig. 2) is the northwestern extension of the Sonnblick Lamella within the Sonnblick Gneiss Dome.

The Möll Valley Fault forms a NW-trending, subvertical topographic and structural lineament, defined by the Möll and the Drau valleys, with a total length of almost 70 km between Obervellach and Villach (Carinthia, Austria) and a dextral offset of the floor thrust between the Penninic and Austroalpine units of *ca* 30 km. Within the Tauern Window it separates the Sonnblick Dome from the Mallnitz Synform (Figs. 2 and 3). To the south, the Sonnblick Dome is bordered by a sinistral ductile to brittle shear zone (Moser Fault) (Fig. 2). This shear zone probably forms a segment of the Defereggen-Antholz-Vals Fault further to the west.

P–T–t data

Rb–Sr white mica ages of *ca* 27 Ma are interpreted to date the maximum temperature of metamorphism within the basement units of the SE sections of the Tauern Window (Reddy *et al.* 1993, Inger & Cliff 1994). Peak metamorphic conditions in gneisses of the Sonnblick area are 540 (+20/−40)° C at 8 ± 1 kbar (Reddy 1989, Reddy *et al.* 1993, Inger & Cliff 1994), and the thermal peak within the neighbouring Hochalm Dome has been reached 3–4 Ma later (Cliff *et al.* 1985). Phase equilibria in rocks of the Lower Schieferhülle indicate peak metamorphic conditions of 500° C at 7 kbar within the western part of the Mallnitz Synform (Droop 1985) and 500° C at 5–6 kbar in the Upper Schieferhülle (Droop 1981). Biotite Rb–Sr ages indicate closure of this isotopic system and cooling through *ca* 300° C between 19 and 23 Ma within the Sonnblick Dome (Reddy *et al.* 1993). Apatite fission track ages document cooling through *ca* 100° C between 8 and 12 Ma within the Sonnblick Dome (Staufenberg 1987). Tension gashes as hydrothermal quartz veins are mineralised with quartz, silicates and sulphides. The sulphides formed at temperatures between 365 and 410° C (Feitzinger & Paar 1991). Reden &

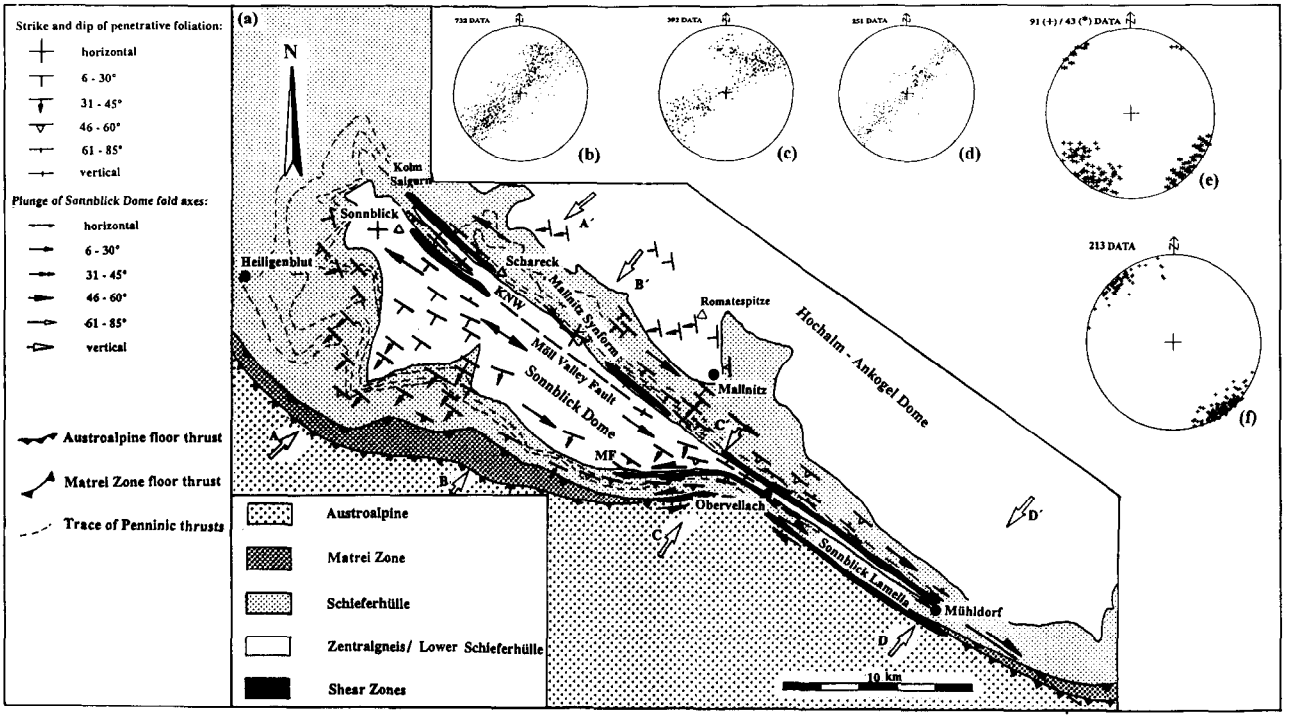

Fig. 2. Simplified tectonic map of the SE Tauern Window and orientation data of penetrative foliation and dome axes. (a) Structure of the Sonnblick Dome as traced by the penetrative foliation (due to nappe stacking) parallel to lithotectonic units; lateral shear zones developed along dome margins; KNW—Knappenhauswalze; MF—Moser Fault. Locations of cross-sections in Fig. 3 are indicated by arrows. (b) Poles to penetrative foliation of the Sonnblick Dome. (c) Poles to penetrative foliation southern part of the Sonnblick Dome. (d) Poles to penetrative foliation of the Mallnitz Synform. (e) Penetrative foliation and stretching lineations within shear zones. (f) Mesoscale fold axes within Sonnblick Dome and Mallnitz Synform. (b–f): Lambert projection, lower hemisphere.

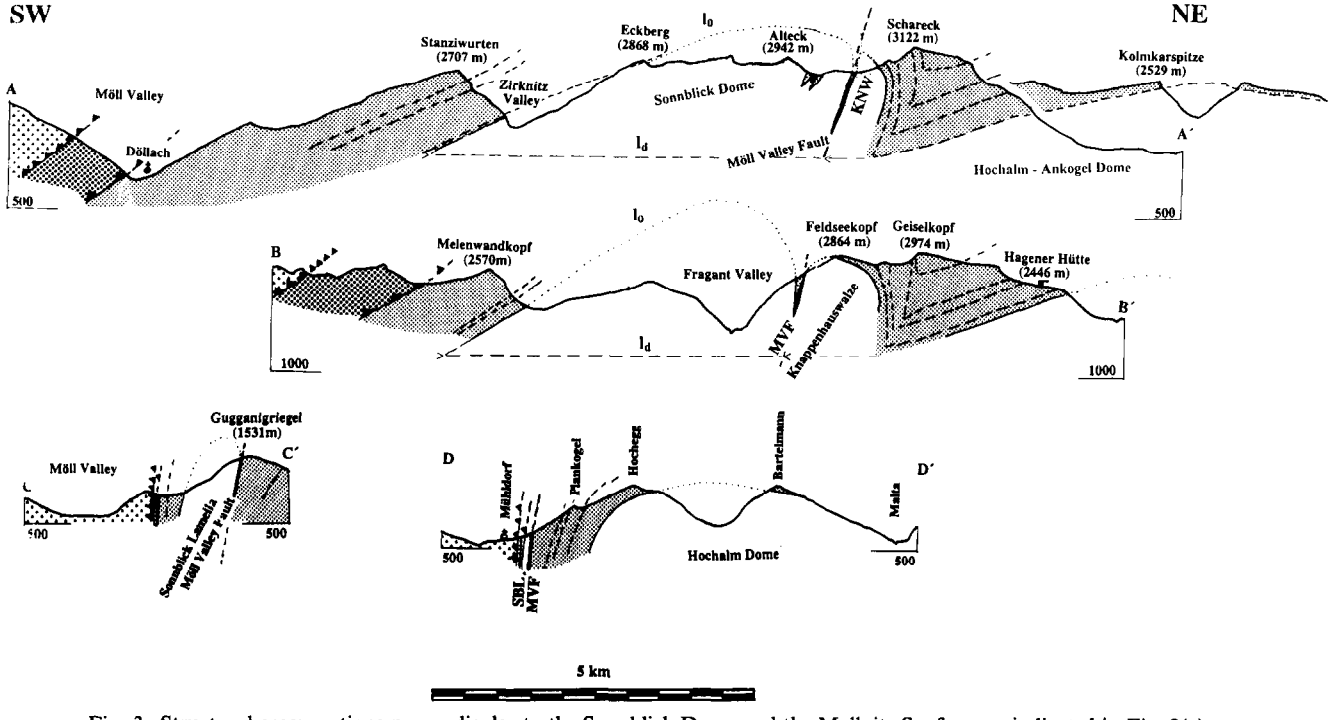

Fig. 3. Structural cross-sections perpendicular to the Sonnblick Dome and the Mallnitz Synform as indicated in Fig. 2(a). KNW—Knappenhauswalze; MVF—Möll Valley Fault; SBL—Sonnblick Lamella. l_0: initial length of exposed section; l_d: deformed length of exposed section of the Sonnblick antiform.

Götzinger (1991) assumed 300° C as a minimum temperature of quartz formation within quartz veins. The *P–T* conditions of vein formation are estimated at $420 \pm 20°$ C and 1.1 ± 0.4 kbar by Droop (1985). Similar data (380° C, 1.3 kbar) are reported by Selverstone *et al.* (1984) and Selverstone & Spear (1985) from the western Tauern Window. If the vein fluids were at lithostatic pressure and in thermal equlibrium with the surrounding rocks, the host rocks must also have experienced the same *P–T* conditions during cooling.

METHODS

We investigated 20 sections perpendicular to the Möll Valley Fault between Mühldorf and Kolm Saigurn across the Sonnblick Dome (Fig. 2). To deduce the sense of movement along the fault we used sense-of-shear-indicators as described, for example, by Bell & Johnson (1992), Simpson & Schmid (1983), Ramsay & Huber (1987), and Hanmer & Passchier (1991). Furthermore, deformation geometry and shear sense are deduced from crystallographically preferred orientation patterns (CPO) of quartz and calcite. In particular calcite-*c*-axis fabrics were used to evaluate the percentage of simple shear and pure shear components in finite deformation (Wenk *et al.* 1987). X-ray goniometry analyses of quartz mylonites were carried out with a Siemens D500 X-ray goniometer at the University of Graz (Austria). The evaluation of pole figures was done using the program TEX11/ODF11 provided by Siemens Co., with corrections for background and angle of inclination. Optical CPOs were measured with a standard universal stage. The orientation of the maximum principal stress, σ_1, from calcite twins and *c*-axes was evaluated using the method described by Dietrich & Song (1984). Slickenside and striae data for paleostress orientation analyses were collected following the methods proposed by Angelier & Mechler (1977) and Angelier (1979), using a computer program as implemented by Wallbrecher & Unzog (1991). Criteria used to determine the sense of slip along brittle faults were described by Petit (1987). Only slickenside and striae data from a single outcrop were used for paleostress orientation analyses to keep control on possible overprinting relationships and multistage formation of faults. Since the data document a distinct single phase of slip along a set of faults, the results more probably document the kinematics and strain axes orientation at a single elaborated station than 'paleostress' orientations (Marret & Allmendinger 1990).

STRUCTURAL DATA AND SEQUENCE OF DEFORMATION

Map geometry and mesoscale structures

The dome structure of the Sonnblick Gneiss Dome is traced by a penetrative foliation ($S_{1,2}$) forming a large NW-trending antiform (Figs. 2 and 3) including subhorizontal fold axes (Fig. 2f). Folds are documented by a girdle distribution of foliation poles $S_{1,2}$ (Fig. 2b–d). The foliation is interpreted to result from ductile deformation during top-to-the-N nappe stacking within Penninic units (D_1) (Kurz *et al.* 1996) which corresponds to D_A^1 of Behrmann (1990) and Droop (1981) and D_A^0 of Bickle & Hawkesworth (1978). Top-to-the-NW ductile shearing was contemporaneous with the thermal peak of Oligocene Barrovian-type metamorphism and homogeneously affected the entire Penninic nappe pile (D_2). This resulted in the development of a second penetrative foliation (S_2) and the transposition of D_1-structures (D_A^2 of Droop 1981, Behrmann 1990). During D_2 the basement units of the Sonnblick Dome were possibly deformed to a large-scale NW-striking fold structure, oriented subparallel to the dominant stretching lineation (Behrmann 1990). The Sonnblick Dome is partly thrusted on to the nappe pile within the Mallnitz Synform, and on to the Hochalm-Ankogel Gneiss Dome along a SW-dipping lateral ramp. Thrusting of the Sonnblick Dome on to the Hochalm-Ankogel Dome is indicated by older cooling ages within the Sonnblick Dome (Reddy *et al.* 1993). Therefore, the Sonnblick anticline was only modified during exhumation and doming. The Austroalpine units along the southern rim of the Tauern Window are crosscut by multiple sets of sinistral and dextral ductile and brittle strike-slip faults which outline small scale triangular blocks and indenters, as exemplified by the Austroalpine block south of Obervellach (Fig. 2).

Confining shear zones

The Sonnblick Dome is bordered by subvertical shear zones along its northeastern and southern margins (Figs. 2 and 3). These shear zones are concentrated along lithological or tectonic boundaries between the Zentralgneis and its hanging-wall units (Figs. 2a and 3), or developed along rheologically weaker zones such as calcareous micaschists and marbles. The first foliation ($S_{1,2}$) is obliterated within these shear zones (D_3) and a new penetrative subvertical foliation (S_3; Figs. 2e, 3 and 4) was developed. Granitic, tonalitic, and aplitic rocks within the Sonnblick Dome suffered chloritization of biotite along these shear zones and brittle faults, up to 1 m away from the shear zone boundaries. The contacts to phyllonitic shear zones are sharp. Along the Sonnblick Lamella a continuous transition from coarse-grained augen gneiss (with potassic feldspar grains of up to 5 cm in the central part) to phyllonites is documented. The phyllonites are characterized by an enrichment of chlorite, phengitic sericite, and quartz at the costs of consumption of potassium feldspar and biotite (Reddy 1989). Within metacarbonates of the Upper Schieferhülle, shear zones can be recognized by a dramatic decrease of the grain size leading to the development of ultramylonites. These shear zones are characterized by a dominant stretching lineation. Subvertical (phyllonitic) shear zones are located mainly along the northeastern and southern margins, between

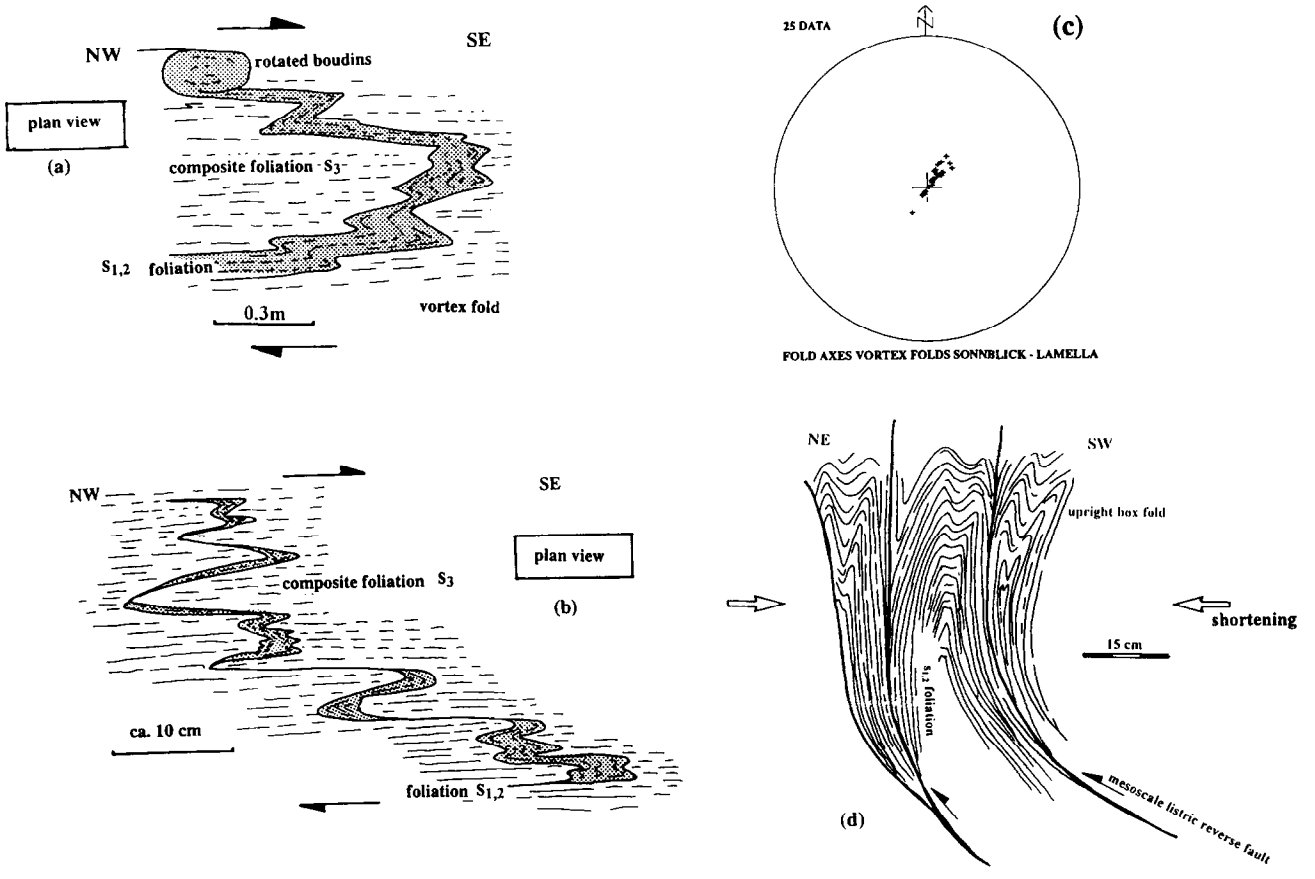

Fig. 4. Plan view of typical vortex fold structures within (a) the Knappenhauswalze and (b) the Sonnblick Lamella. (c) Orientation data of vortex fold axes. (d) Box folds within calcareous schists along the southern margin of the Sonnblick Dome.

the Sonnblick antiform and the Knappenhauswalze, and the Sonnblick Lamella, respectively, and are folded around NW-trending axes (Figs. 2 & 3). The width of these shear zones significantly increases at the highest exposed structural levels. A prominent stretching lineation along the shear zones plunges gently (5–15°) to the SE (Fig. 2e). The geometrical arrangement of the conjugate dextral and sinistral shear zones implies NE- to NNE-directed subhorizontal contraction.

Mesoscale structures within the Sonnblick Dome and the Sonnblick Lamella

The dominant mesoscale structures within and along the Sonnblick Lamella and the Knappenhauswalze are isoclinal folds with subvertical axes (b_3) (Figs. 4a–c). These folds are sometimes developed as shear folds documenting a clockwise rotational deformation component. These are the earliest mesoscale features indicating subhorizontal NE- to NNE-directed contraction oblique to the Sonnblick Dome combined with a dextral sense of shear. These structures dominate within and along the Sonnblick Lamella, and its extension in the Knappenhauswalze (Fig. 2). The penetrative foliation and subsequently injected, minor discordant quartz veins, are folded (D_3), which results in the formation of a composite foliation together with the pre-existing penetrative foliation ($S_{1,2}$). The asymmetry of these folds decreases continuously to the SE along the Sonnblick Lamella. Stretch values (l_d/l_0) of folded discordant veins of up to 0.7 occur within the Knappenhauswalze and the Sonnblick Lamella. However, this is only an approximation because deformation is mainly ductile.

The following structures affected the D_1–D_3 fabrics and are mostly restricted to the interior of the Sonnblick Dome. Along the southern margin of the Sonnblick Dome and the southeastern margin of the Sonnblick Lamella, the penetrative foliation (S_{1-3}) is affected by upright and southwestward overturned box folds (D_{4a}), with NW-trending fold axes (Fig. 4d). Subvertical sulphide-bearing crack–seal quartz veins of centimetre to decimetre thickness and narrow chlorite-bearing fissures are the oldest brittle structures (D_{4b}). They trend NE, perpendicular to the fold axes of the Sonnblick Dome, and show a right-lateral en-echelon arrangement (Figs. 5a & f). These structures dominate the hinge and the central regions of the Sonnblick anticline and occur within the Hochalm-Ankogel Dome. They are less pronounced along the southern and southwestern margins of the Sonnblick Dome. At the highest structural levels of the Sonnblick Dome, earlier structures are affected by open to tight NE-vergent recumbent folds. Along the southern margin the folds are partly SW-vergent. These folds are characterized by an axial planar crenulation cleavage (D_{4c}) (Figs. 5a & g) which is defined

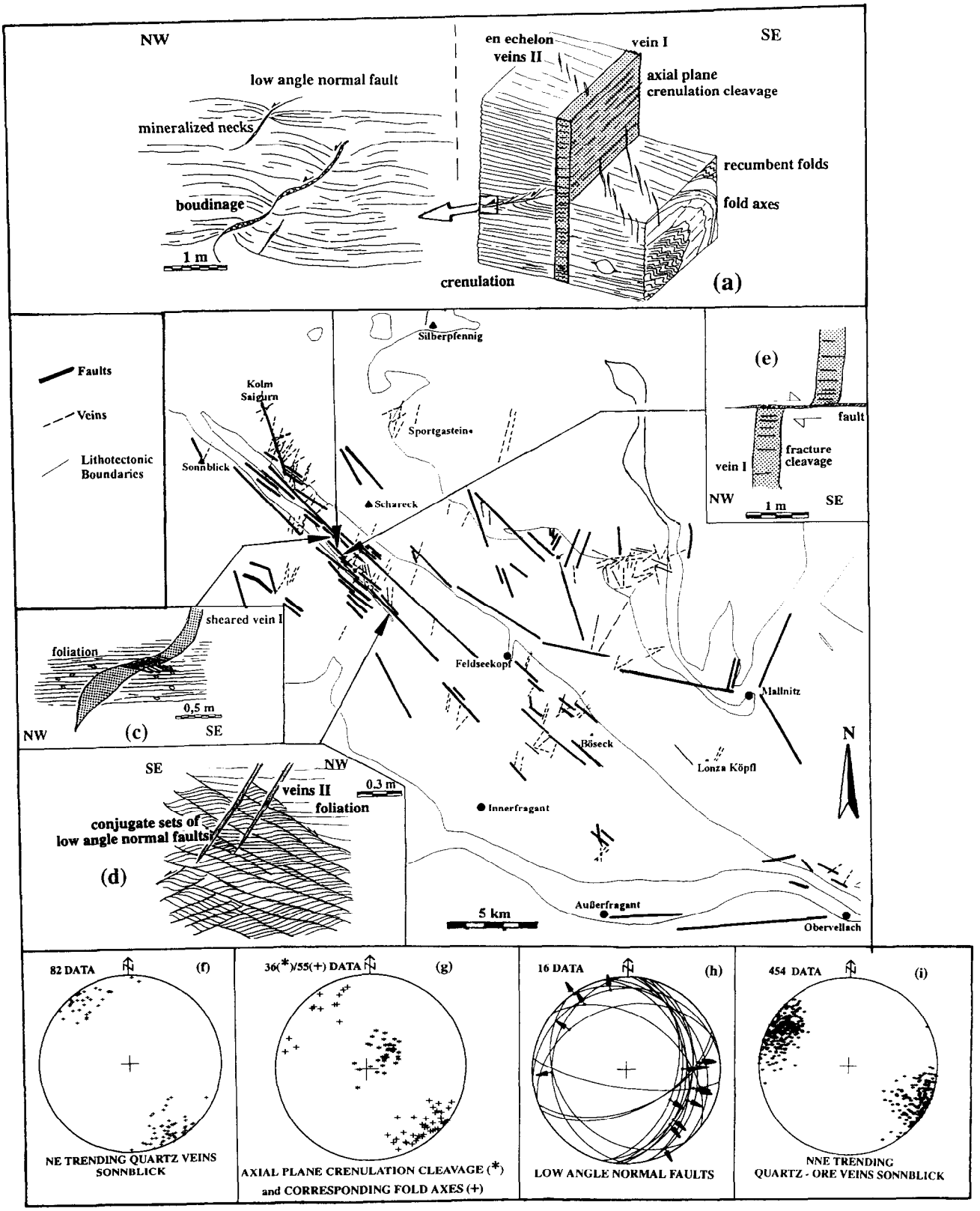

Fig. 5. (a–e) Location and structural position of doming-related structures (D_4) within the Sonnblick Dome with map scale traces of most important faults and Au-quartz veins and compilated remote sensing lineaments (faults and most important Au-quartz veins). (f) NE-trending gold bearing quartz veins I. (g) Subhorizontal axial planar crenulation cleavage and related fold axes. (h) Representative low-angle normal faults and striae from the central part of the Sonnblick Dome. (i) Orientation data of gold-bearing sulphidic quartz veins II. (g–i) Lambert projection, lower hemisphere.

by newly developed white mica. The steeply SW-dipping axial plane of the Sonnblick Dome and the $S_{1,2,3}$ composite foliation along the Knappenhauswalze and the Sonnblick Lamella are affected by this deformation, too. This indicates shortening in a subvertical direction, and hence folding on flat-lying axial surfaces. These recumbent folds can also be distinguished from the fold structures developed during the upbending of the Sonnblick Dome by the orientation of their axial surfaces. The latter are subvertical or dip steeply to the SW within the Sonnblick Dome and the Sonnblick Lamella.

All structures mentioned above are crosscut by sets of low-angle normal faults in middle and upper structural levels dipping to the WNW and ESE, respectively (D_{4d}; Figs. 5a, b & h). The low-angle normal faults form conjugate sets on a mesoscale, in particular in higher structural sections (Figs. 5d & h), and single SE-dipping sets on the macroscale. Extensional veins are sheared and offset by these low-angle normal faults (Fig. 5c). Linear fabrics on the fault planes plunge to the E to SE (Fig. 5h). Locally an asymmetric foliation boudinage (Platt & Vissers 1980) is related to single sets of low-angle normal faults (Fig. 5b). The NE-trending veins, the folds and the low-angle normal faults are crosscut by NNE-trending extensional quartz–sulphide veins ('Tauern-gold quartz-veins') (D_{4e}; veins II in Figs. 5a, d & i). The NNE-trending veins are associated with brittle NW-trending faults, parallel to the Möll Valley Fault (Fig. 6a), and with synthetic R-shears (D_{4e}). These veins are often concentrated within overlapping fault segments. Older, NE-trending quartz veins are reactivated as antithetic left-lateral brittle faults (R'-shears). The NNE-striking veins are arranged in a dextral en-echelon pattern when they are linked with main NW-trending faults (Y-shears) or with R-shears, and in a sinistral en-echelon pattern when they are linked with R'-shears. Older, NE-trending quartz veins, are furthermore offset in a right-lateral sense of shear by NW-trending subvertical brittle faults and they also show a fracture cleavage subparallel to these faults (Fig. 5e). Both types of veins are subsequently activated as high-angle normal faults or are crosscut by NW- to WNW-dipping high-angle normal faults.

Contemporaneous to the formation of NNE-trending veins (D_{4e}), the subvertically oriented northeastern limb of the Sonnblick Dome including its confining shear zones, and the Sonnblick Lamella are brittlely reactivated. The results of paleostress analyses based on fault-slip data along the Möll Valley Fault and along the southern margin of the Sonnblick Dome indicate a subhorizontal NNE–SSW orientation of the principal stress σ_1 while slip was active along these faults (Fig. 6b). This orientation of σ_1 is compatible with the formation of NNE-trending extensional veins (Figs. 6a & b). σ_3 was oriented ESE–WNW. Outside the Möll Valley Fault as well as in the central and the hinge region of the Sonnblick Dome, σ_1 was oriented subvertically while σ_3 remained in an ESE–WNW orientation (Fig. 6b). Only along the southern margin of the Sonnblick Dome was σ_3 oriented N–S at one station (Fig. 6b). Some of the NNE-trending veins are subsequently used as high-angle normal faults (Fig. 6a) (D_{4f}), which document an exchange of σ_1 and σ_2 outside of the Möll Valley Fault (Kurz *et al.* 1994).

D_3 microstructures and microfabrics

Shear criteria, as shear bands and extensional crenulation cleavage (ecc; Figs. 7a–d) document predominantly dextral displacement along the northeastern margin of the Sonnblick Gneiss Dome (Möll Valley Fault). Locally antithetic sinistral shear bands are developed. Along E–W striking shear zones (Moser Fault), sinistral displacement is documented.

Within the Zentralgneis of the Sonnblick Dome and the Mallnitz Synform, quartz completely recrystallized after the development of the penetrative foliation ($S_{1,2}$), as indicated by equigranular grains with diameters of 0.2 to 0.5 mm and straight grain boundaries, forming triple junctions. Crystallographic axes show a strong preferred orientation (Kurz 1993). At the borders of the dome, quartz is characterized by strongly elongated grains with aspect ratios of 3:1 up to 5:1, highly undulatory extinction and subgrains. Core–mantle-fabrics are locally developed due to subgrain rotation recrystallization (Figs. 7a & b). The diameter of recrystallized grains is about 0.05 mm. Quartz domains between multiple sets of shear bands often display equigranular grains which are slightly affected by deformation (Figs. 7a & b). Calcite mylonites within the shear zones contain less than 5% quartz and mica. Calcite displays uniform grain size between 0.3 and 1 mm. It is homogeneously twinned with conjugate sets of twins developed (Fig. 7c). Twins are often bent due to intracrystalline plasticity of calcite within micro-scale shear zones, while domains between conjugate shear band sets are less deformed. Core–mantle textures are occasionally recognized (Fig. 7c). Approaching the Austroalpine units along the SW margin of the Sonnblick Lamella and the S margin of the Sonnblick Dome, ultramylonites with optically not-discernable calcite grains are developed within the shear zones. Along the shear zones confining the dome structure, a continuous transition from plastic to brittle fabrics, including the development of cataclasites within quartz- and feldspar-rich rocks, is documented (Riedmüller & Schwaighofer 1970, 1971). Quartz grains are affected by extensional cracks which are filled mainly with calcite. This calcite is deformed by twinning (Fig. 7c) and pressure solution.

Crystallographic Preferred Orientation (CPO)

Quartz *c*-axis distributions of samples taken from phyllonitic shear zones display slightly oblique type I crossed girdles with one stronger girdle developed (Fig. 8). They document right-lateral shearing along the northeastern margin of the Sonnblick Dome (Möll Valley Fault), and left lateral shearing along its southern

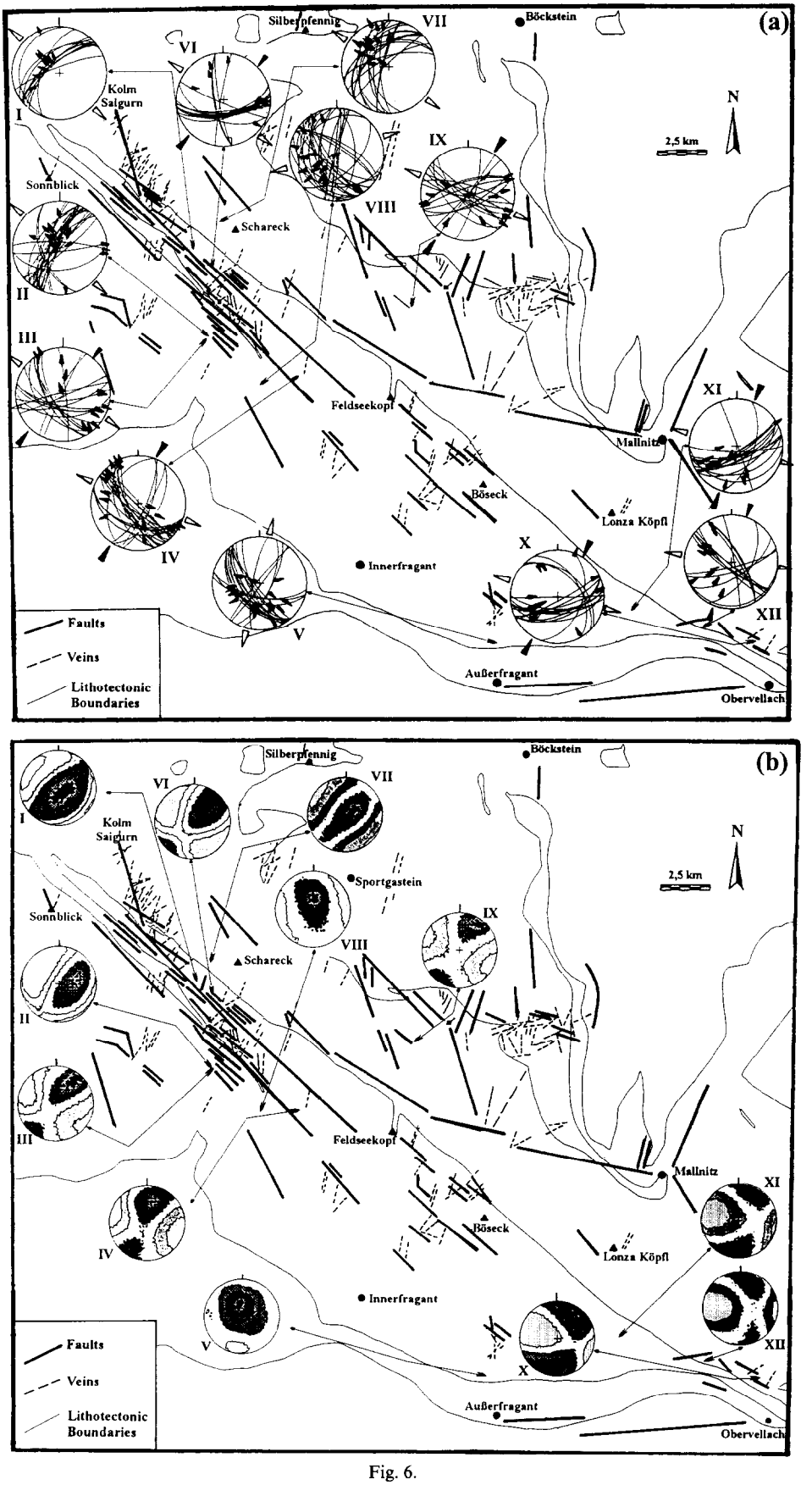
(a)
Silberpfennig
Böckstein
VI
VII
Kolm Saigurn
I
IX
N
2,5 km
Sonnblick
VIII
Schareck
II
III
Feldseekopf
XI
Mallnitz
Böseck
Lonza Köpfl
IV
Innerfragant
X
XII
V
Faults
Veins
Lithotectonic Boundaries
Außerfragant
Obervellach
(b)
Silberpfennig
Böckstein
VI
VII
I
Kolm Saigurn
N
2,5 km
Sportgastein
Sonnblick
IX
VIII
Schareck
II
III
Feldseekopf
Mallnitz
XI
Böseck
IV
Lonza Köpfl
Innerfragant
V
X
XII
Faults
Veins
Lithotectonic Boundaries
Außerfragant
Obervellach

Fig. 6.

margin (Moser Fault) (Fig. 8). The type I crossed girdles progressively develop to small circle distributions along the Möll Valley fault and the Sonnblick Lamella. The results of the quartz *c*-axis data are corroborated by calcite *c*-axis data from calcite–mylonitic shear zones, and the orientation of the maximum principal stress σ_1 (Fig. 9) evaluated from calcite twin/*c*-axis pairs. Along the Sonnblick Lamella and the NE margin of the Sonnblick Dome, calcite *c*-axes cluster close to the short axis of the finite strain ellipsoid (Z) with a fabric asymmetry ω of 1.5–2.5° (Fig. 10), where ω describes the asymmetry of the CPO-maxima to the shear zone boundary and the pole to the shear plane, respectively (Wenk *et al.* 1987). Along the southern margin of the Sonnblick Dome ω ranges from 11° to 23°. Following Wenk *et al.* (1987), this implies a component of simple shear of up to 10% along NW-trending dextral shear zones (Möll Valley Fault), and between about 35% and 70% along W-trending sinistral shear zones (Moser Fault) (Fig. 10), assuming that the samples are pure marble mylonites, and the mylonitic foliation within the shear zones approximates the shear zone boundaries. This assumption can be justified by the high finite strains in the investigated samples. The orientation data of maximum principal stress axes evaluated from calcite *c*-axes and *e*-twin pairs display subhorizontal N- to NNE-directed shortening along confining shear zones and within the Mallnitz Synform during the final stages of updoming (Fig. 9). Sample 193/2 (Fig. 9) indicates NW-directed shortening.

DISCUSSION

The shape of the Sonnblick Dome is related to folding of the tectonic units including an earlier penetrative foliation, which originated from ductile thrusting. Folding leads to the formation of an asymmetric, NE-vergent dome. The Sonnblick Dome is bordered by wide, steep shear zones; these are (1) the dextral Möll Valley Fault and the Sonnblick Lamella along its NE margin and (2) the sinistral Moser Fault along its southern margin. Oblique shortening relative to pre-existing surfaces and structures resulted in development of these discrete shear zones along the boundaries of the upbending dome. The complex deformation patterns along the dome margins document heterogeneous deformation and strain partitioning (Platt 1984) within an approximately constant external stress regime. Non-coaxial flow is localized within these shear zones and along associated low-angle normal shear zones along the upper margins of the gneiss dome. However, major portions of the dome remained largely unaffected by non-coaxial flow. Within these parts only semiductile and brittle structures, like veins and recumbent folds, dominate, accommodating coaxial flow.

Partitioning of transpressional deformation can occur when stress is applied oblique to pre-existing zones of structural weakness (Jones & Tanner 1995). Zones of structural weakness include lithological contacts and rheological heterogeneities (e.g. the subvertical contact between the gneisses of the Sonnblick Dome and the metasediments within the Mallnitz Synform). Other zones of weakness are pre-existing faults or shear zones situated within the deformation zone or along its boundaries (e.g. the Möll Valley Fault). These shear zones within the Sonnblick area developed during deformation at decreasing temperatures.

The Sonnblick Lamella is the first site along the Möll Valley Fault where non-coaxial ductile deformation is concentrated during a decrease in temperature. The Sonnblick Lamella is best interpreted as a stretching fault (Means 1989, 1990) segment of the Möll Valley fault. The stretching fault segment evolved progressively from SE to NW along the Möll Valley Fault, including the Knappenhauswalze (Figs. 2 and 3). The amount of horizontal shortening along this dextral fault is difficult to estimate. Veins folded during D_3 locally indicate subhorizontal stretch (l_d/l_0) of 0.5–0.7. Lateral displacement along the Möll Valley Fault can be estimated from the offset of the Austroalpine floor thrust and is in the order of 25 km (Fig. 12c). Lateral displacement decreases continuously to the northwestern tip of the Möll Valley Fault and is in the order of 2.5 km at the tip of the Knappenhauswalze (Fig. 2), evaluated by the lateral displacement between the Sonnblick Dome and the Hölltor-Rotgülden Dome (Fig. 1). Sub-vertical NNE-trending en-echelon veins II (Figs. 5a, d & i) are concentrated at the end of the Möll Valley Fault and within extensional jogs of overlapping fault segments. This suggests formation of these structures within an accommodation zone at the tip of the fault, which partly compensated for the dextral strike-slip component by ESE-directed extension and vein formation (Kurz *et al.* 1994). One possible explanation for the shortening recorded in the Sonnblick Dome and its resultant narrowing from a few kilometres to only 100–300 m is the indentation of an Austroalpine crustal wedge, outlined by the dextral Möll Valley Fault and the conjugate sinistral Moser Fault (Fig. 12). A simple schematic model for the thermal and structural evolution during the development of the Sonnblick Dome is presented in

Fig. 6. (a) Fault planes and striae orientation data and compilated remote sensing lineaments from the area of the Sonnblick Dome, lineaments from Holzer (1958a,b), Cliff *et al.* (1971), Feitzinger & Paar (1991) and Feitzinger (1992) as well as field-mapped faults and veins; dark arrows at the margins of the pole figures indicate the approximate orientation of σ_1, light arrows σ_3. (b) Paleostress (strain) orientation data deduced from faults within single exposures presented in Fig. 6(a); black or dark grey: maximum densities of compression axes obtained from single fault-slip measurements; light grey: calculated orientation of σ_3. **I**: WK 163, 12 data, Max.: 12, Min.: 0; **II**: WK 199, 31 data, Max.: 30, Min.: 1; **III**: WK 200, 19 data, Max.: 18, Min.: 1; **IV**: WK 353, 27 data, Max.: 27, Min.: 0; **V**: WK 351, 22 data, Max.: 22, Min.: 0; **VI** WK 168, 18 data, Max.: 18, Min.: 0; **VII**: WK 205, 18 data, Max.: 18, Min.: 0; **VIII**: WK 181, 36 data, Max.: 27, Min.: 9; **IX**: WK 339, 19 data, Max.: 19, Min.: 0; **X**: WK 24, 18 data, Max.: 17, Min.: 1; **XI**: WK 256, 15 data, Max.: 15, Min.: 0; **XII**: WK 1, 14 data, Max.: 13, Min.: 1.

Figs. 11 and 12. From the orientation of veins II we can assume a NNE direction of contraction (20°; Fig. 12c). The amount of horizontal shortening at the tip of the indenter amounts to *ca* 5.2 km, as indicated by the geometrical arrangement of the Möll Valley Fault, the shortening direction, and the lateral displacement of the Austroalpine floor thrust. Similar values (*ca* 5.5 km) can be estimated from the dome antiform itself, by subtracting the deformed length (l_d), which is exposed across the Sonnblick Dome, from the initial length (l_0) in a cross-section perpendicular to the dome structure (Fig. 3). The jump in metamorphic grade between the orthogneiss of the Sonnblick Lamella ($\pm$8 kbar, 540–560° C) and rocks of the Peripheral Schieferhülle ($\pm$6 kbar, 500° C) that are in tectonic contact along the Möll Valley Fault, indicates *ca* 6 km shortening, assuming a geobarometric gradient of 0.3 kbar per km^{-1}. The en-echelon veins II are not, or only slightly, affected by further deformation and, therefore, reflect the orientation of the incremental principal strain axes during the final stage of dome formation. Reddy *et al.* (1993) alternatively suggested that despite its vergence to the NE, the antiform results from dominantly NW-directed tectonic transport, with the dominant structure caused by movement over a SW-dipping oblique or lateral blind thrust ramp (Fig. 12d) prior to peak thermal metamorphism within the Sonnblick area. This might also explain the fact that metamorphic isograds appear not to be folded around the Sonnblick Dome axis (Droop 1981, 1985). The Sonnblick antiform may have been rotated passively around its NW-trending axis during subsequent doming and exhumation of the Hochalm-Ankogel Dome (Fig. 12d). In this scenario, the antiform within the Sonnblick Dome was modified by pushing it towards the Austroalpine crustal wedge to the SW which resulted in the development of the Sonnblick Lamella and the Möll Valley Fault.

Deformation partitioning is developed on all scales in the area. For example, *c*-axis orientations were mainly measured within domains between multiple sets of shear bands where a higher amount of simple shear has been accommodated. The evaluation of simple shear percentage from the preferred orientation of calcite-*c*-axes (Figs. 9 & 10) is therefore only a minimum estimate. Accordingly, the same feature is indicated by quartz *c*-axis distributions (Fig. 8), especially in polyphase aggregates, while pure quartz samples seem to express higher simple shear percentages than polyphase aggregates. Furthermore, the orientation of the maximum principal stress axis σ_1, from the orientation of calcite *c*-axes and twins (Fig. 9), reflects the final increment of deformation (Dietrich & Song 1984) within pure calcite samples. From the angle between the pole to foliation plane (shear zone boundary) and σ_1, the percentage of simple shear may be calculated with respect to the shear zone boundary. This depends on the orientation of a pre-existing surface (Weijermars 1991), e.g. the penetrative foliation or a fault. The progressive change of quartz *c*-axis distributions from type I crossed girdles to small circles from NW to SE along the Möll Valley Fault and the Sonnblick Lamella might reflect a relative increase of the pure shear component to the SE, but it may also reflect decreasing temperature (and, therefore, different crustal levels). Similarly, transformation of feldspars into hydrous minerals like phengitic sericite within these shear zones may have resulted in work softening (Reddy 1989).

Furthermore, within this area, a transition from vertical thickening to vertical thinning along the eastern margin of the Tauern Window can be observed. Transpression with vertical escape (Sanderson & Marchini 1984) dominates within the Sonnblick Dome, while transpression and lateral escape (Dias & Ribeiro 1994) around the tip of the indenter resulted in the formation of the Sonnblick Lamella (Fig. 12b). Vertical thinning is documented by a low-angle normal fault zone confining the Tauern Window to the east (Genser & Neubauer 1989). The Möll Valley fault marks this transition zone from vertical thickening to thinning and forms the lateral southwestern boundary of this low-angle normal fault detachment. Normal displacement along this detachment is transferred into lateral displacement along the Möll Valley Fault. Footwall uplift with a normal fault system, that acted within a transpressional regime, contributed to the rapid, nearly isothermal exhumation of the dome structure. According to the published age data and the documented structural evolution, exhumation started already prior to peak thermal conditions within the Sonnblick Dome. Following Reddy *et al.* (1993) the deformation style changed from shortening to extension prior to biotite closure at *ca* 19 Ma (Fig. 11a). Brittle deformation still occurred at elevated temperatures, as documented by hydrothermal mineral assemblages within fissures linked with the Möll Valley Fault. Thus, brittle failure along the Möll Valley Fault seems to be highly dependent on very high strain rates and fluid pressure. *P–T* and geochronological data indicate rapid, nearly isothermal exhumation, with very high exhumation rates of up to 5 mm per year (Cliff *et al.* 1985), and rather high cooling rates after decompression had ceased (Fig. 11b). The duration of exhumation, unroofing, and doming along the Möll Valley Fault is difficult to estimate since the main part of the fault is covered by Quaternary glacial deposits. While a clear discordance exists in K–Ar cooling ages between the Penninic realm and Austroalpine units along the Möll Valley Fault, this discordance is not recorded by fission track ages (Staufenberg 1987, Hoke 1990). This implies that the highest amount of dip-slip displacement along the Möll Valley Fault occurred between 20 and 10 Ma. There is general agreement that the Möll Valley Fault is reactivated as a conjugate dextral Riedel shear to the Periadriatic Lineament in the Miocene (Schmid *et al.* 1989, Polinski & Eisbacher 1992). However, this is based only on the feasible geometric arrangement, not on investigation on the fault itself. The indenter along the south-eastern margin of the Tauern Window (Fig. 12) seems to be coupled to the large Southalpine Indenter confined by the Periadriatic Lineament and the Giudicarian Line.

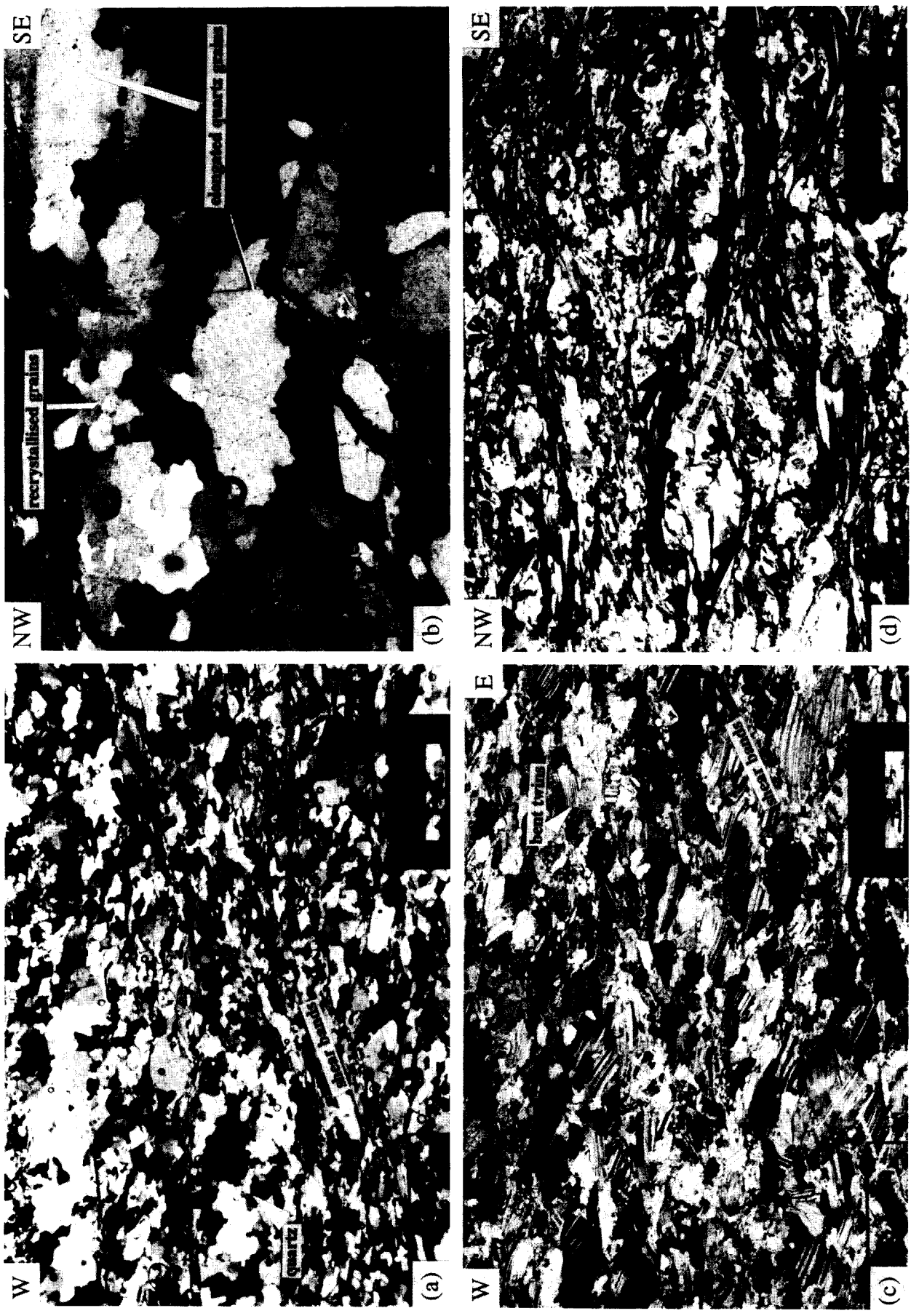

Fig. 7. Representative microfabrics from subvertical shear zones along dome margins. (a) Quartz fabric and shear bands along the southern margin of the Sonnblick Dome; shear bands document sinistral displacement along steep foliation. (b) Quartz fabric within high strain domains along shear bands. (c) Calcite fabrics and shear bands along the southern margin of the Sonnblick Dome; shear bands document sinistral displacement. (d) Shear bands document dextral displacement along the Möll Valley Fault. Cross-polarized optical micrographs. Width of photomicrographs (a), (b) and (d) is 4 mm, and of (c) is 1.5 mm.

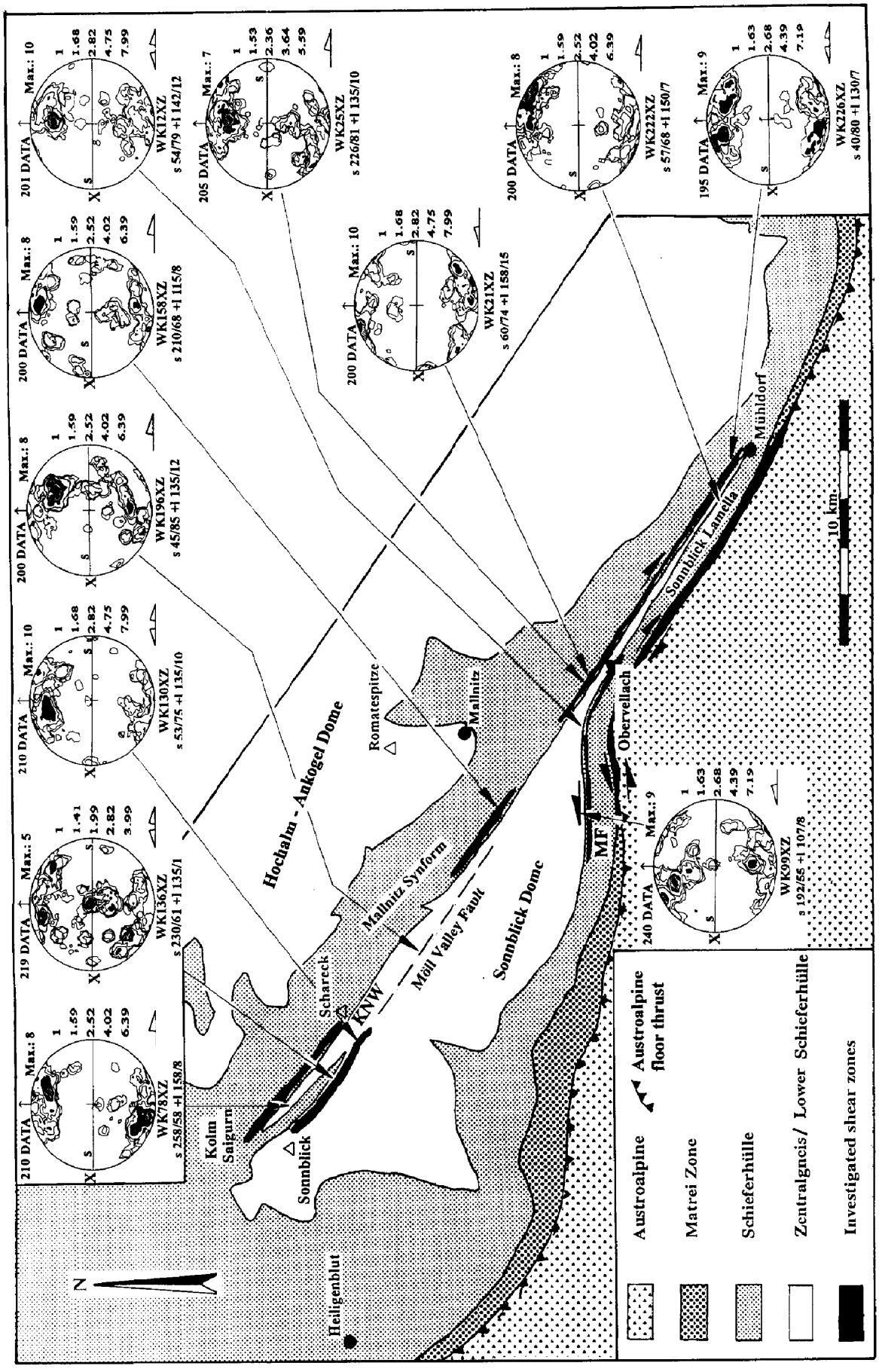

Fig. 8. Sketch map of the southeastern Tauern Window with location and diagrammatic presentation of quartz CPOs along the northeastern and southern margins of the Sonnblick Dome and Sonnblick Lamella, respectively. The orientation of the penetrative foliation and the stretching lineation and the sample number is given for each specimen. Values at the right margin of each diagram document Multiples of Random Distribution (MRD) for the areas bordered by isolines. 'Max.'— values (black and dark gray) indicate MRD within the *c*-axes maximum.

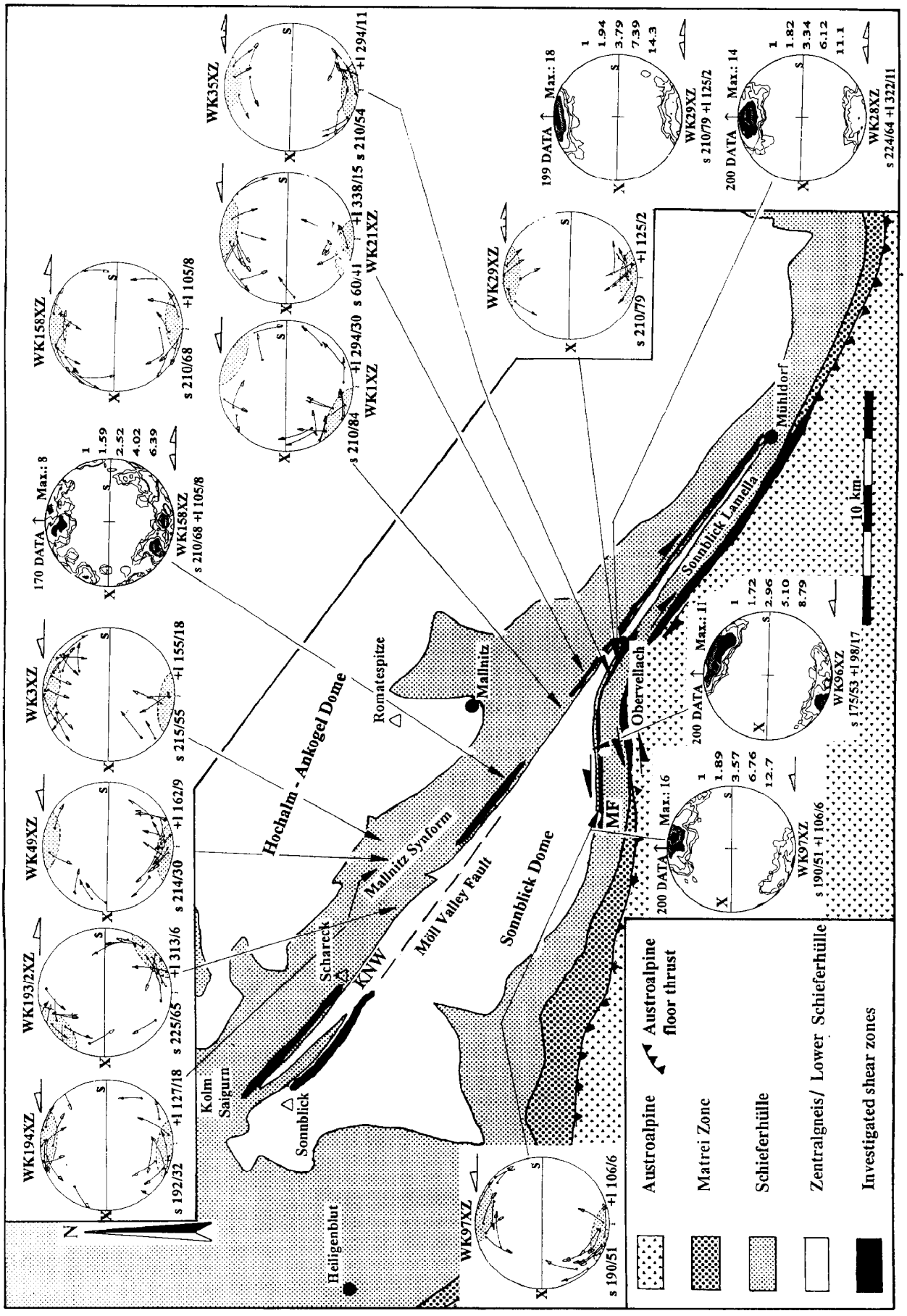

Fig. 9. Calcite: *c*-axis distributions (for explanation see Fig. 8) and orientation data of maximum principal stress from the orientation of e-twins and c-axes from shear zones and from the Mallnitz Synform according to the method of Dietrich & Song (1984). Points: *c*-axes; arrows: poles of twin planes; stippled area: possible orientation of σ_1.

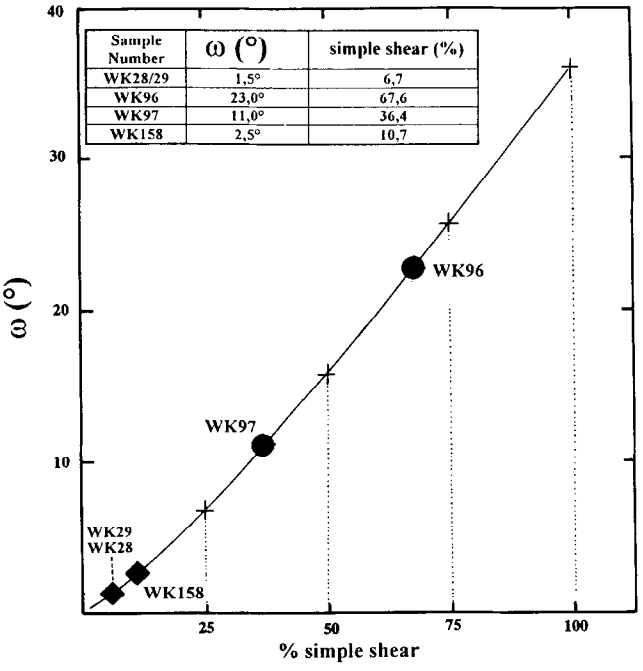

Fig. 10. Diagrammatic representation of percentage of simple shear deduced from calcite *c*-axes data for five samples (WK28XZ, WK29XZ, WK96XZ, WK97XZ, WK158XZ) along shear zones (diagram according to Wenk *et al.*, 1987); ω: angle between the [0001] maximum and the pole to the shear plane; ◆ dextral shear zones parallel to the Möll Valley Fault; • sinistral shear zones along the southern margin of the Sonnblick Dome.

Dome-forming mechanisms

Several mechanisms may contribute to doming of a metamorphic core complex within a contractional regime: (1) upbending of previously subhorizontal thrust surfaces; (2) ductile flattening strain with a subvertical oblate finite strain ellipsoid; and (3) a dip-slip-component along strike-slip faults bordering the upbending dome resulting in the development of a oblique-ramp anticline. Thickening and doming resulted in subvertical flattening of the highest structural section of the dome structure, documented by recumbent folds with a subhorizontal axial plane and subhorizontal crenulation cleavage (Fig. 12d) and low-angle normal faults at a more advanced stage of doming. Thus, during its development, the dome structure passed a neutral, isotropic stress surface. Crossing this surface caused the swapping of the principal stresses σ_1 and σ_2, while σ_3 remained constant in orientation. Only along the southern margin of the Sonnblick Dome was σ_3 locally oriented N–S. This could be an indication of equality of σ_2 and σ_3 and undirected gravitational collapse (Gamond 1987). The exchange of the intermediate and largest principal paleostress axes is interpreted as the result of increased gravitational forces which arose as the consequence of surface uplift. This gravitational force did overcome the subhorizontal forces due to push from the indenter and it did overcome the strength of the rocks (Ratschbacher *et al.* 1989). The exchange is documented by the development of low angle-normal faults in middle and higher structural levels of the surface uplifting dome as well as in vertical shortening, removal of the overburden, and unroofing (Genser & Neubauer 1989, Neubauer & Genser 1990, Ratschbacher *et al.* 1989) until the horizontal principal stresses (due to push from the indenter) overcame vertical stresses again. A second cycle of principal stress exchange is documented in the development of brittle strike-slip faults along pre-existing surfaces and associated extensional quartz veins which have subsequently been activated as high-angle normal faults. Analyses of fault slip data (Fig. 6) are compatible with the development of extensional veins. The orientation of contraction is constant during dome formation. From the opposite point of view, subhorizontal contraction may dominate as long as it is released by slip along subvertical strike-slip faults, and subvertical maximum principal stresses related to gravitational forces and overburden are subsequently released.

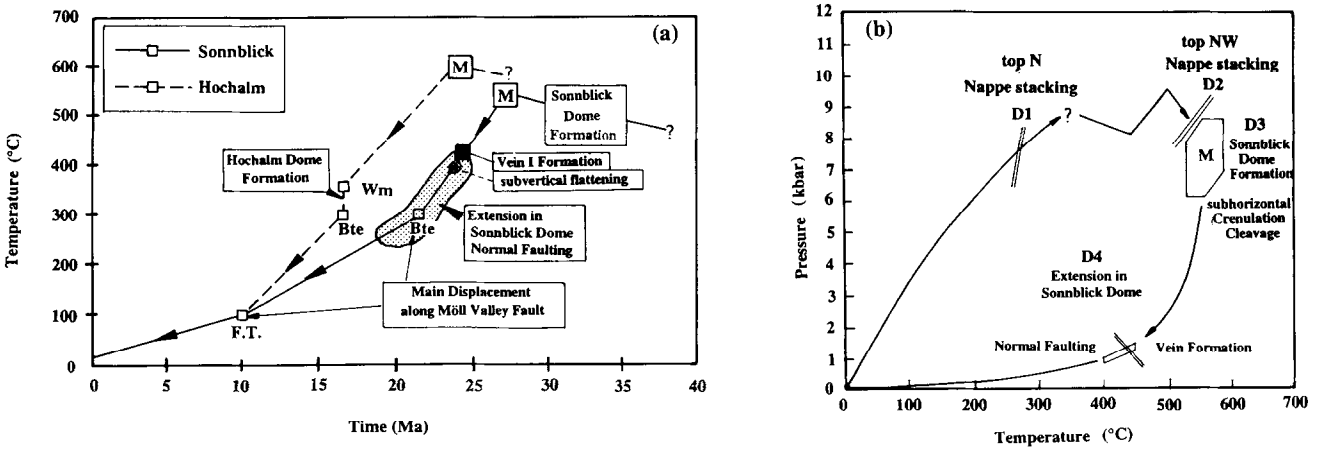

Fig. 11. Temperature–pressure–time-deformation paths for the Sonnblick Dome and the Hochalm Dome with time calibrations of doming-related structures based on petrological and geochronological data after Reddy *et al.* (1993), Cliff *et al.* (1985) and Droop (1985). (a) Temperature–time path after Reddy *et al.* (1993) with sequence of deformation events (this study). (b) *P–T* path for the base of the Schieferhülle near Obervellach during Alpine deformation after Droop (1985) with sequence of deformation events (this study). M: Metamorphism, thermal peak; white mica Rb–Sr ages from the Sonnblick Dome near M; Wm–K: Ar white mica data Hochalm Dome. Bte: Rb–Sr biotite data. F.T.: Apatite fission track data.

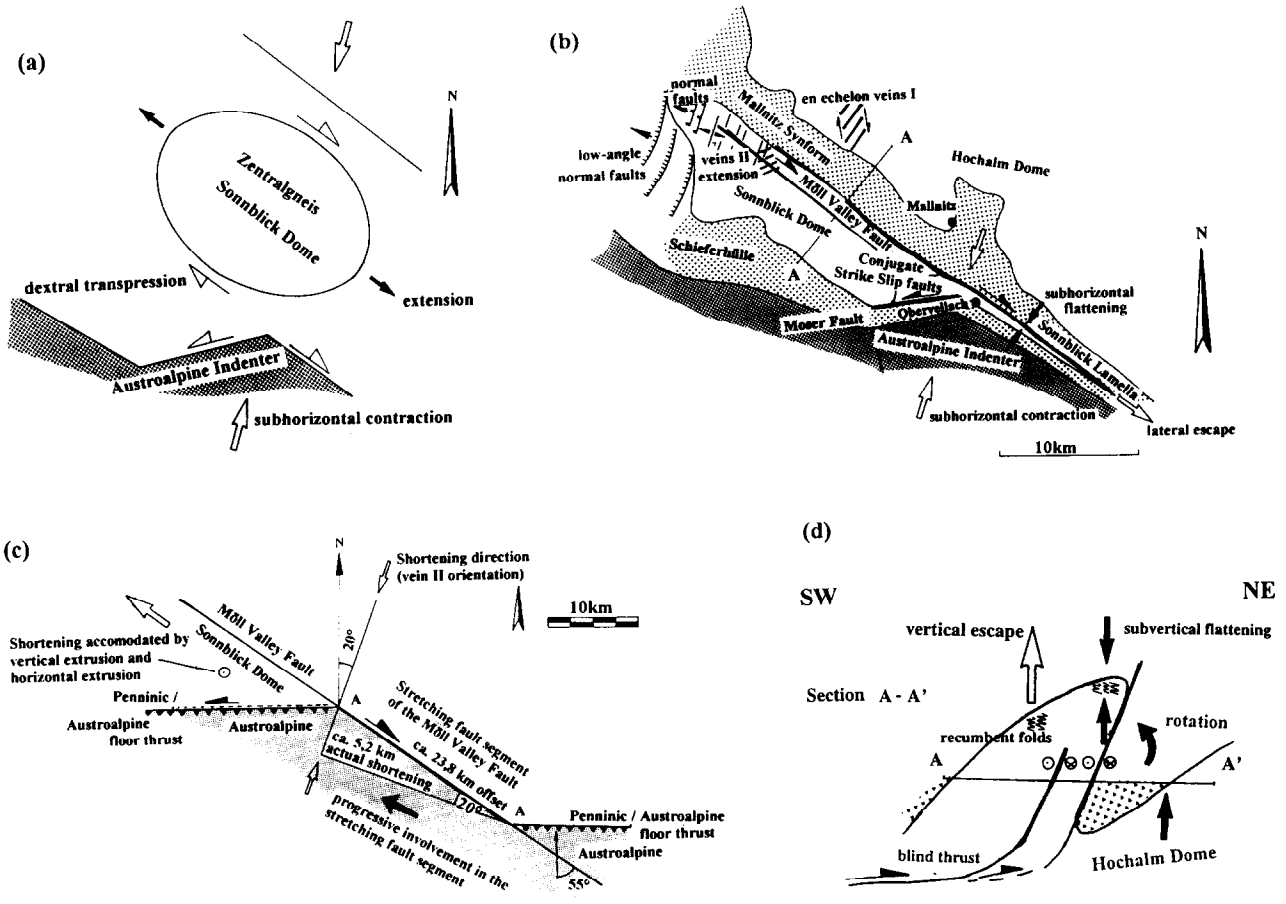

Fig. 12. Simplified model for the evolution of the SE Tauern Window during doming with development of significant structures during different stages of doming; for clarity only structures for each stage of dome evolution are represented. (a) Possible 'initial' stage and state. (b) Final stage and state and major structures. (c) Simplified geometric reconstruction and estimation of horizontal shortening and lateral dextral displacement along the Möll Valley fault and the Sonnblick Lamella from the geometrical arrangement of the Möll Valley Fault segment, the Austroalpine indenter, assuming a NNE direction of horizontal contraction. (d) Simplified cross-section perpendicular to the Sonnblick Dome from Fig. 12(b) with development of significant structures during doming.

Acknowledgements—We appreciate discussions on the topics presented in this study with Simon Hanmer, Mark Handy, Reiner Kleinschrodt, Justus Krawinkel and many others who participated in the field trip during the meeting of 'Structures and Tectonics at Different Lithospheric Levels'; in Graz in September '93. We further appreciate field discussions with Niko Froitzheim and Neil Mancktelow. Special tribute to Hans Genser who is one of the creators of the exhumation model for the Tauern Window and to Kurt Stüwe, Ewald Hejl, and Robert Handler who contributed a lot of critical remarks. We also gratefully acknowledge the computer programs of Eckard Wallbrecher and Wolfgang Unzog for numerical calculations of 'paleostress' data. Special thanks to Fritz Finger who allowed us to investigate his 'Hohe Tauern Batholith'. Final studies and the preparation of this paper have been carried out within the project P9918-GEO of the Austrian Research Foundation. We gratefully acknowledge very careful reviews by Lothar Ratschbacher, Giles T. R. Droop and Cees W. Passchier.

REFERENCES

Angelier, J. 1979. Determination of the mean principal direction of stresses for a given fault population. *Tectonophysics* **56**, T17–T26.

Angelier, J. & Mechler, P. 1977. Sur une methode graphique de recherche des contraintes principles egalement utilisable en tectonique et en seismologie: la methode des diedre droits. *Bull. Soc. geol. Fr.* **19**, 1309–1318.

Behrmann, J. H. 1988. Crustal scale extension in a convergent orogen: the Sterzing–Steinach mylonite zone in the Eastern Alps. *Geodinamica Acta* **2**, 63–73.

Behrmann, J. H. 1990. Zur Kinematik der Kontinentkollision in den Ostalpen. *Geotekt. Forsch.* **76**, 1–180.

Behrmann, J. H. & Frisch, W. 1990. Sinistral ductile shearing associated with metamorphic decompression in the Tauern Window, Eastern Alps. *Jahrb. Geol. Bundesanst.* **133**, 135–146.

Bell, T. H. & Johnson, S. E. 1992. Shear sense: a new approach that resolves conflicts between criteria in metamorphic rocks. *J. met. Geol.* **10**, 99–124.

Bickle, M. J. & Hawkesworth, C. J. 1978. Deformation phases and tectonic history of the eastern Alps. *Bull. geol. Soc. Am.* **89**, 293–306.

Christensen, J. N., Selverstone, J., Rosenfeld, J. L. & DePaolo, D. J. 1994. Correlation by Rb–Sr geochronology of garnet growth histories from different structural levels within the Tauern window, Eastern alps. *Contr. Miner. Petrol.* **118**, 1–12.

Cliff, R. A., Droop, G. T. R. & Rex, D. C. 1985. Alpine metamorphism in the south-east Tauern Window, Austria: II. heating, cooling and uplift rates. *J. met. Geol.* **3**, 403–415.

Cliff, R. A., Norris, R., Oxburgh, E. R. & Wright, R. C. 1971. Structural, metamorphic and geochronological studies in the Reisseck and southern Ankogel Groups. *Jahrb. Geol. Bundesanst.* **114**, 121–272.

Coney, P. J. 1980. Cordilleran metamorphic core complexes: An overview. *Mem. geol. Soc. Am.* **153**, 7–35.

Davies, G. H. 1983. Shear-zone model for the origin of metamorphic core complexes. *Geology* **11**, 342–347.

Dewey, J. F. 1988. Extensional collapse of orogens. *Tectonics* 7, 1123–1139.

Dias, R. & Ribeiro, A. 1994. Constriction in a transpressive regime: an example in the Iberian branch of the Ibero–Armorican arc. *J. Struct. Geol.* **16**, 1543–1554.

Dietrich, D. & Song, H. 1984. Calcite fabrics in a natural shear environment, the Helvetic nappes of western Switzerland. *J. Struct. Geol.* **6**, 19–32.

Droop, G. T. R. 1981. Alpine metamorphism of pelitic schists in the south-east Tauern Window, Austria. *Schweiz. Miner. Petrogr. Mitt.* **61**, 237–273.

Droop, G. T. R. 1985. Alpine metamorphism in the south-east Tauern Window, Austria: I. P–T variations in space and time. *J. met. Geol.* **3**, 371–402.

England, P. & Molnar, P. 1990. Surface uplift, uplift of rocks and exhumation of rocks. *Geology* **18**, 1173–1177.

Exner, Ch. 1962. Sonnblicklamelle und Mölltallinie. *Jahrb. Geol. Bundesanst.* **105**, 273–286.

Exner, Ch. 1964. Erläuterungen zur Geologischen Karte der Sonnblickgruppe 1: 50. 000. *Geol. Bundesanst., Vienna*, 170 pp.

Feitzinger, G. 1992. Gold–Silber—Vererzungen und historischer Bergbau im Zirknitz- und Wurtental (Sonnblickgruppe, Hohe Tauern, Kärnten). *Lapis* **13**, 13–30.

Feitzinger, G. & Paar, W. H. 1991. Gangförmige Gold-Sibervererzungen in der Sonnblickgruppe (Hohe Tauern, Kärnten). *Arch. Lagerst. forsch. Geol. Bundesanst.* **13**, 17–50.

Gamond, J. F. 1987. Bridge structures as sense of displacement in brittle fault zones. *J. Struct. Geol.* **9**, 609–620.

Genser, J. & Neubauer, F. 1989. Low angle normal faults at the eastern margin of the Tauern window (Eastern Alps). *Mitt. Österr. geol. Ges.* **81**, 233–243.

Hanmer, S. & Passchier, C. 1991. Shear sense indicators: a review. *Geol. Surv. Can.* Paper 90-17, 72 pp.

Hill, E. J. & Baldwin, L. 1993. Exhumation of high-pressure metamorphic rocks during crustal extension in the D'Entrecasteaus region, Papua, New Guinea. *J. met. Geol.* **11**, 261–277.

Hill, J., Baldwin, S. L. & Lister, G. S. 1992. Unroofing of active metamorphic core complexes in the D'Entrecasteaux Islands, Papua, New Guinea. *Geology* **20**, 907–910.

Hoke, L. 1990. The Altkristallin of the Kreuzeck Mountains, SE Tauern Window, Eastern Alps—Basement Crust in a Convergent Plate Boundary Zone. *Jahrb. Geol. Bundesanst.* **133**, 5–87.

Holzer, H. F. 1958a. Photogeologische Karte eines Teiles der Goldberggruppe. *Jahrb. Geol. Bundesanst.* **101**, 25–34.

Holzer, H. F. 1958b. Zur photogeologischen Karte der Kreuzeckgruppe. *Jahrb. Geol. Bundesanst.* **101**, 187–190.

Inger, S. & Cliff, R. A. 1994. Timing of Metamorphism in the Tauern Window, Eastern Alps: Rb–Sr-ages and fabric formation. *J. met. Geol.* **12**, 695–707.

Jones, R. & Tanner, P. W. G. 1995. Strain partitioning in transpression zones. *J. Struct. Geol.* **17**, 793–802.

Kurz, W. 1993. Strukturentwicklung längs der Mölltallinie (südöstliches Tauernfenster). *Unpublished MSc. Thesis*, University of Graz, 246 pp.

Kurz, W., Neubauer, F. & Genser, J. 1996. Kinematics Penninic nappes (Glockner Nappe and basement-cover nappes) in the Tauern Window (Eastern Alps, Austria), during subduction and Penninic–Austroalpine collision. *Eclogae Geol. Helv.* **89**, 573–605.

Kurz, W., Neubauer, F., Genser, H. & Horner, H. 1994. Sequence of Tertiary brittle deformations in the eastern Tauern Window (Eastern Alps). *Mitt. Österr. geol. Ges.* **86**, 153–164.

Lister, G. S., Banga, G. & Feenstra, A. 1984. Metamorphic core complexes of Cordilleran type in the Cyclades, Aegean Sea, Greece. *Geology* **12**, 221–225.

Lister, G. S. & Davis, G. A. 1989. The origin of metamorphic core complexes and detachment faults formed during Tertiary continental extension in the northern Colorado River region, U.S.A. *J. Struct. Geol.* **11**, 65–94.

Malavielle, J. 1987. Kinematics of compressional and extensional ductile shearing deformation in a metamorphic core complex of the northeastern Basin and Range. *J. Struct. Geol.* **9**, 541–554.

Marret, R. & Allmendinger, R. W. 1990. Kinematic analyses of fault slip data. *J. Struct. Geol.* **12**, 973–986.

Means, W. D. 1989. Stretching faults. *Geology* **17**, 893–896.

Means, W. D. 1990. One dimensional kinematics of stretching faults. *J. Struct. Geol.* **12**, 267–272.

Neubauer, F., Dallmeyer, D., Dunkl, I. & Schirnik, D. 1995. Late Cretaceous exhumation of the metamorphic Gleinalm dome, Eastern Alps: kinematics, cooling history, and sedimentary response in a sinistral wrench corridor. *Tectonophysics* **242**, 79–98.

Neubauer, F. & Genser, J. 1990. Architektur und Kinematik der östlichen Zentralalpen—eine Übersicht. *Mitt. naturwiss. Ver. Stmk.* **120**, 203–219.

Petit, J. P. 1987. Criteria for the sense of movement on fault surfaces in brittle rocks. *J. Struct. Geol.* **9**, 597–608.

Platt, J. P. 1984. Secondary cleavages in ductile shear zones. *J. Struct. Geol.* **6**, 439–442.

Platt, J. P. 1986. Dynamics of orogenic wedges and the uplift of high-pressure metamorphic rocks. *Bull. geol. Soc. Am.* **97**, 1037–1053.

Platt, J. P. 1993. Exhumation of high-pressure rocks: a review of concepts and processes. *TERRA Nova* **5**, 119–133.

Platt, J. P. & Vissers, R. L. M. 1980. Extensional structures in anisotropic rocks. *J. Struct. Geol.* **2**, 397–410.

Polinski, R. K. & Eisbacher, H. 1992. Deformation patitioning during polyphase oblique convergence in the Karawanken Mountains, southeastern Alps. *J. Struct. Geol.* **14**, 1203–1213.

Ramsay, J. G. & Huber, M. I. 1987. *The Techniques of Modern Structural Geology, Volume 2: Folds and Fractures.* Academic Press, London.

Ratschbacher, L., Frisch, W., Linzer, H. G. & Merle, O. 1991. Lateral Extrusion in the Eastern Alps. Part 2: Structural Analysis. *Tectonics* **10**, 257–271.

Ratschbacher, L., Frisch, W., Neubauer, F., Schmid, S. M. & Neugebauer, J. 1989. Extension in compressional orogenic belts: The eastern Alps. *Geology* **17**, 404–407.

Reddy, S. M. 1989. The interaction of deformation and metamorphic processes within ductile shear zones in the Zentralgneis complex Austria. *Terra Abstracts* **1**, 380.

Reddy, S. M., Cliff, R. A. & East, R. 1993. Thermal history of the Sonnblick Dome, south-east Tauern Window, Austria: Implications for Heterogenous uplift within the Pennine basement. *Geol. Rdsch.* **82**, 667–675.

Reden, G. & Götzinger, M. 1991. Fluid inclusions in vein mineralisations in the region of Badgastein, Rauris and Heiligenblut (Hohe Tauern/ Austria). *Ann. Meeting IGCP Project no. 291 "Metamorphic fluids in mineral deposits", Zürich, March 21–23*, Abstracts, 47–48.

Riedmüller, G. & Schwaighofer, B. 1970. Mineralumwandlungen in Myloniten der Oschenikseestörung (Kärnzen, Österreich). *Mitt. Ges. Geol. Bergbaustud. österr.* **19**, 315–328.

Riedmüller, G. & Schwaighofer, B. 1971. Elektronenoptische Untersuchungen von Kaoliniten aus Myloniten der Oschenikseestörung (Kärnen, österreich). *Carinthia II SH.* **28**, 253–258.

Sanderson, D. J. & Marchini, W. R. D. 1984. Transpression. *J. Struct. Geol.* **6**, 449–458.

Schmid, S. M., Aebli, H. R., Heller, F. and Zingg, A. The role of the Periadriatic Line in the tectonic evolution of the Alps. In: Alpine Tectonics (edited by Coward, M. P., Dietrich, P. & Park, R. G.) *Spec. Publs. geol. Soc. Lond.* **45**, 153–171.

Selverstone, J. 1985. Petrologic constraints on imbrication, metamorphism, and uplift in the SW Tauern Window, Eastern Alps. *Tectonics* **4**, 687–704.

Selverstone, J. 1988. Evidence for east–west crustal extension in the Eastern Alps: implications for the unroofing history of the Tauern window. *Tectonics* **7**, 87–105.

Selverstone, J. 1993. Micro- to macroscale interactions between deformational and metamorphic processes, Tauern Window, Eastern Alps. *Schweiz. mineral. petrogr. Mitt.* **73**, 229–239.

Selverstone, J., Morteani, G. & Staude, J. M. 1991. Fluid channeling during ductile shearing: transformation of granodiorite into aluminous schist in the Tauern Window, Eastern Alps. *J. Met. geol.* **9**, 419–431.

Selverstone, J. & Spear, F. S. 1985. Metamorphic *P–T* Paths from pelitic schists and greenstones from the south-west Tauern Window, Eastern Alps. *J. met. Geol.* **3**, 439–465.

Selverstone, J., Spear, F. S., Franz, G. & Morteani, G. 1984. High-Pressure Metamorphism in the SW Tauern Window, Austria: *P–T* Paths from Hornblende–Kyanite–Staurolite Schists. *J. Petrol.* **25**, 501–531.

Simpson, C. & Schmid, S. M. 1983. An evaluation of criteria to deduce the sense of movements in sheared rocks. *Bull. geol. Soc. Am.* **94**, 1281–1288.

Staufenberg, H. 1987. Apatite fission-track evidence for postmetamorphic uplift and cooling history of the eastern Tauern Window and the surrounding Austroalpine (Central Eastern Alps, Austria). *Jahrb. Geol. Bundesanst.* **130**, 571–586.

Tollmann, A. 1977. Die Geologie von österreich (Band I): Die Zentralalpen. Deuticke, Vienna, 766 pp.

Wallbrecher, E. & Unzog, W. 1991. GEFUEGE 4 (Version 4. 1): Ein Programmpaket zur Behandlung von Richtungsdaten. Dept. of Geology, University of Graz.

Weijermars, R. 1991. The role of stress in ductile deformation. *J. Struct. Geol.* **13**, 1061–1078.

Wenk, H. R., Takeshita, T., Bechler, E., Erskine, B. & Mathies, S. 1987. Pure shear and simple shear calcite textures. Comparison of experimental, theoretical and natural data. *J. Struct. Geol.* **9**, 731–745.